 doi:10.20944/preprints202002.0188.v1

Article

Interfacial Phenomena between Liquid Si-Rich Si-Zr Alloys and Glassy Carbon

Donatella Giuranno [1,2]*, Wojciech Polkowski[2], Grzegorz Bruzda[2], Artur Kudyba[2], Javier Narciso[3,4]*

[1] Institute of Condensed Matter Chemistry and Energy Technologies (ICMATE), National Research Council of Italy (CNR),Via De Marini 6, Genoa, 16149, Italy; donatella.giuranno@ge.icmate.cnr.it
[2] Łukasiewicz Research Network - Foundry Research Institute, Zakopiańska 73 Str., 30-418 Krakow, Poland wojciech.polkowski@iod.krakow.pl; artur.kudyba@iod.krakow.pl; grzegorz.bruzda@iod.krakow.pl
[3] Instituto Universitario de Materiales de Alicante (IUMA), Universidad de Alicante, Apdo. 99, Alicante, 03080, Spain; narciso@ua.es
[4] Departamento de Química Inorgánica, Universidad de Alicante, Apdo. 99, Alicante, 03080, Spain;

* Correspondence: donatella.giuranno@ge.icmate.cnr.it; narciso@ua.es

Abstract:

To design and optimize liquid-assisted processes such as reactive infiltration for fabricating refractory SiC/$ZrSi_2$ composites, basic investigations on the interfacial phenomena occurring when liquid Si-based alloys are in contact with C and SiC substrates, are key steps. Indeed, targeted wettability studies may provide helpful indications for finding the suitable set of operating conditions to succeed the fabrication of composites via the reactive infiltration and for predicting the key influencing mechanisms.

The wettability of glassy carbon (GC) by two different Si-rich Si-Zr alloys as a function of the Si-content has been investigated by the sessile drop method at T = 1450°C. The more relevant results obtained in terms of equilibrium contact angle values, spreading kinetics, reactivity and developed interface microstructures are reported in the paper and compared with the behaviour previously observed in the Si-27Zr/GC system. The increase of Si-content only weakly affected the overall phenomena observed at the interface, which from the practical point of view means that even the Si-Zr alloys with higher Si-content, as respect to the eutectic alloy (Si-27Zr), could be potentially used as infiltrant materials.

Keywords: MMCs; Silicon Carbide; Wetting; Refractory materials; Zr-Silicides.

1. Introduction

At the present, SiC/SiC_f, C_f/SiC and SiCp (SiC particles reinforced) composites densified or filled by Si-based alloys as well as transition metal silicides, are gaining great interest as thermal barriers and structural materials or components for assembling re-entry space vehicles and fission/fusion nuclear reactors for their low density, remarkable hardness, chemical inertness, high electrical and thermal stability, excellent resistance to oxidation, particularly at high temperatures [1-8]. For instance, refractory alloys and silicides, such as Zr-based alloys and Zr combined with Si are already used as cladding materials for nuclear reactors because of their ultra-high neutron capture cross sections and an excellent long-term resistance under irradiation [8-12].

To design and produce such composites with tailored properties, the Reaction Bonded/Formed Silicon Carbide process, belonging to spontaneous/pressure-less infiltration mechanisms, has well known advantages over other conventional and costly sintering techniques, namely lower processing temperatures, shorter times and near-net shape fabrication capabilities [13-17]. In fact, SiC/$ZrSi_2$

composites have been already successfully produced by the reactive infiltration of three different liquid Si-rich Si-Zr alloys into bi-modal SiC preforms [18]. An excellent thermal compatibility between the metal phase and SiC reinforcement without any evidence of debonding phenomena or residual stresses, as well as a low CTE, were resulting by the thermo-mechanical characterization performed on the as-produced SiC/$ZrSi_2$ composite.

As reported in the literature, the reactive infiltration was also used to produce C_f/ZrC–SiC composites having outstanding ablation and erosion resistance even at temperatures higher than T = 1600 °C were produced by infiltrating C felt preforms by liquid Si-8.8 at% Zr eutectic and Si-10 at% Zr hypo-eutectic alloys [19-22]. To limit the C-dissolution phenomenon, in both cases the C-fibers were previously coated with pyrolytic carbon by a chemical vapour deposition process. As a further confirmation, liquid metal infiltration is currently used to fabricate SiC-fiber–reinforced Si-based eutectic alloys composites, which are currently under developement for aerospace applications. Specifically, Si-16at%Ti, Si-17at%Cr, Si-22at%Co, Si-38at%Co, and Si-27at%Fe alloys. The mentioned Si-based alloys are investigated as infiltrants of amorphous SiC-fibers with C as the interface layer for improving the overall oxidation resistance at high temperatures. In particular, the excellent oxidation resistance can be successfully predicted using thermodynamic calculations, as it has been documented in [23].

In order to succeed in designing and manufacturing such composites, key contributions could be coming from fundamental investigations of thermodynamic and thermophysical properties of the melt phase, such as surface properties, density, viscosity [24-26]. In parallel, the wetting characteristics and reactivity at the alloy/preform interfaces ought to be evaluated [27-32]. The as collected knowledge can be profitably used as an input for optimizing the infiltration process [16, 33].

In order to provide new knowledge on the interaction phenomena occurring when a liquid Si-rich Si-Zr alloy is in contact with C or SiC based materials, a careful experimentally-based study was done by analysing the behaviour of liquid Si-10at% Zr near eutectics alloy in contact with both amorphous C (i.e. GC-Glassy Carbon) [31] and Hot-Pressed polycrystalline silicon carbide (HP-SiC) [32]. Namely, wettability, reactivity, as well as the overall interfacial phenomena observed at the interfaces were analysed and related to the operating conditions.

To scale up the reactive infiltration process from the lab to industrial scale, several affecting factors should be taken into consideration. Specifically, the starting metal materials may suffer the presence of impurities and a more pronounced inhomogeneity in the alloy composition, usually resulting in a high amount of Si segregation and the resulted surface oxidation. Additionally, the temperature imposed to infiltrate the alloy into the preform is usually around T = 1450 °C with a heating rate around 5°C/min or even slower. Consequently, being the selected infiltrants lower-melting Si-based alloys (i.e. near eutectic composition), the infiltration process may start at temperatures lower than T = 1450 °C. Moreover, if the starting material differs from the nominal composition, not homogeneus and anomaolous melting due to the presence of large amount of pure Si, is expected.

For this reason, the influence of Si-content on the interfacial phenomena occurring between Si-Zr system and the GC was investigated by the contact heating sessile drop method at T = 1450 °C and the main relevant results are reported in the present paper.

In order to check the reliability of the results obtained, the contact angle behaviours observed on the GC for the two Si-rich Si-Zr alloys investigated were compared with the experimental observations provided from wetting tests previously performed on pure Si and Si-10at%Zr in contact with the GC under the same operating conditions and by applying the same experimental procedure.

The microstructure characterization of the interfaces by Light Microscopy (OM) and Scanning Electron Microscopy (SEM) combined with an Energy Dispersive X-Ray analyser (EDS), was done.

For the sake of clarity, the scope of the paper is to highlight how the wetting (the key property for infiltration processes) studies may provide useful information to optimize the infiltration in terms of operating parameters.

In other words, by focusing on interfacial phenomena in terms of adhesion, reactivity, growth of reaction layers, etc., some factors negatively affecting the reactive infiltration process, (i.e. the pore

Preprints (www.preprints.org) | NOT PEER-REVIEWED | Posted: 14 February 2020 doi:10.20944/preprints202002.0188.v1

narrowing/pore closure and fibers-degradation by C-dissolution) can be easily predicted and limited to a great extent.

2. Materials and Methods

Glassy Carbon (GC) provided by Alfa-Aesar was used with as received surface conditions. A surface roughness of Ra ≈ 20 nm on a GC area of 3x3 mm^2 was measured by an optical confocal-interferometric profilometer (Sensofar S-neox).

The Si-Zr alloys samples were prepared by mixing high purity (99.98%-Goodfellow®), mechanically cleaned and the weighted Si and Zr pieces, that were melted by an arc melting furnace under an atmosphere of high purity Ar. In order to reduce the residual oxygen content inside the arc-melting chamber, a Zr drop (acting as O_2-getter) was previously melted. To ensure the homogeneity of the alloy composition, each Si-Zr sample (having initial mass of ≈ 0,05 g) was re-melted 3 times. By checking the final weight of the alloy samples, no evidences of evaporation or material loss were revealed. The microstructure and composition of as produced Si-Zr alloys at the cross-sectioned sample were checked by SEM/EDS, as shown in Figure 1.

As it can be seen, a two-phase of Si+$SiZr_2$ segregated at the Si-grain boundaries was detected both in the bulk of Si-1.7at%Zr and Si-5.3at%Zr alloy samples (i.e. Si-5wt%Zr and Si-15wt%Zr, hereafter denoted as Si-5Zr and Si-15Zr). The predominance of the Si+$SiZr_2$ phase depends on the Si-content, as expected.

In both cases, a layer of pure Si was found segregated at the surface of alloy drop. Contrarily, pure Si and $ZrSi_2$ were detected at the surface of the Si-10at%Zr alloy sample (from now Si-27Zr). Moreover, $ZrSi_2$ precipitates embedded into the eutectic matrix with a Zr-content varying from 8.15 to 9 at%, were revealed at the bottom of the drop.

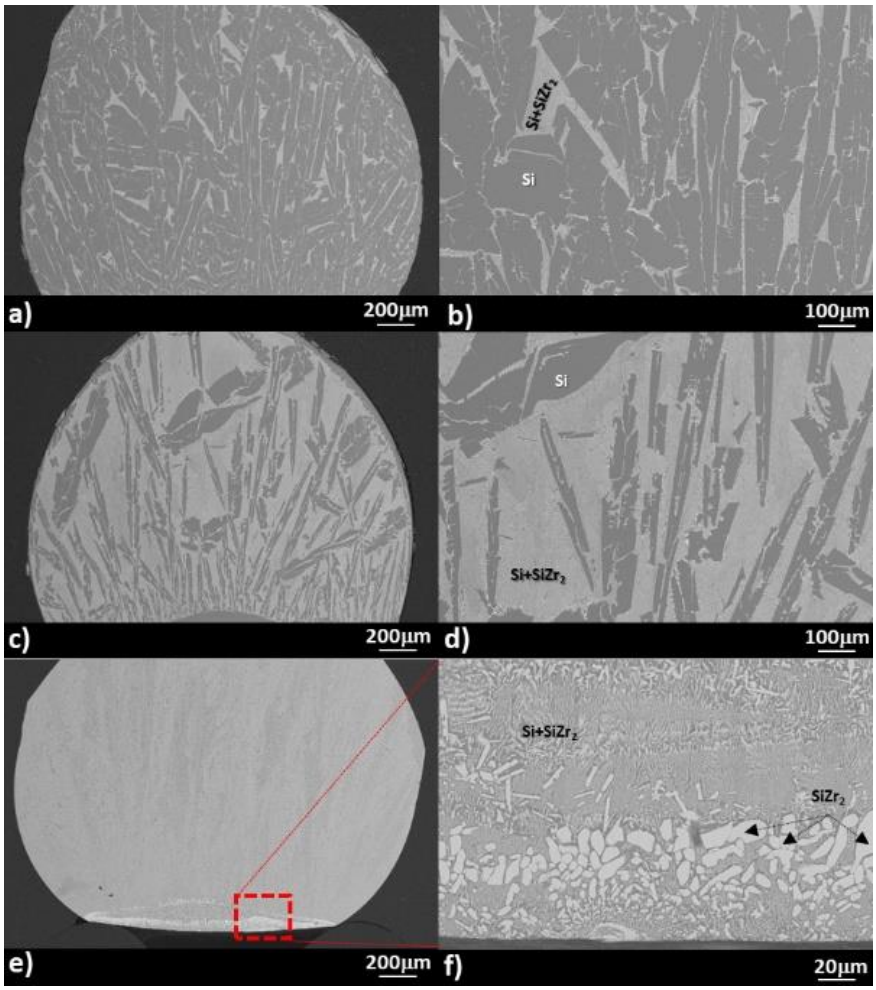

 doi:10.20944/preprints202002.0188.v1

Figure 1. BSE/EDS analyses performed at two magnifications at the cross-sectioned as-produced alloys samples: (**a**) and (**b**) Si-5Zr; (**c**) and (**d**) Si-15Zr; (**e**) and (**f**) Si-27Zr.

Prior to the wetting experiments, the Si-Zr alloy sample and the substrate were weighted, rinsed in an ultrasonic bath and dried with compressed air.

The Si-Zr/GC assembly was placed on a graphite sample holder, located at the central part of the heater and leveled at the horizontal plane.

In order to remove any contaminant from the experimental environment, the device was outgassed under vacuum conditions ($P_{tot} \leq 10^{-6}$ mbar) for two hours.

The alloy /substrate couple was heated (at the rate of 10 °C/s) by an 800 kHz high frequency generator coupled to a porous graphite tube (Figure 2a), which provides an atmosphere with reduced oxygen content.

To limit evaporation phenomena, wetting experiments were performed under a static Ar atmosphere ($O_2 < 0.1$ ppm) and following the procedure detailed elsewhere [27].

The evolution of the contact angle values over time was monitored in real-time and recorded (10 frames/sec) by a high resolution CCD-camera connected to a computer.

Every single frame was processed by an image analysis software ad hoc-developed (ASTRAVIEW®) [34] allowing automatic acquisition of the contact angle values and drop geometric variables (R-base radius and H-drop height). By analyzing the experimental method used and all the factors that can affect measured contact angle value, the accuracy of the data obtained is estimated to be around ± 2° [35].

After the wetting experiments, the samples were cold-embedded in epoxy-resin, cross-sectioned, metallographically polished and prepared for the microstructural characterization by LM and SEM/EDS techniques.

3. Results

Figure 2 shows the wetting behavior of the liquid Si in contact with the GC substrate at T = 1450 °C. In particular, by analyzing both the variation of contact angle as a function of time and the sequence of images recorded during the first 25 s of the wetting test, an anomalous behavior during the Si melting was observed (Figure 2a). After 25 s from the start of the isothermal step, the complete melting of Si was reached and a contact angle value of $\theta = 70°$ was measured at the Si/GC triple line. In the following 60 s, the steady state condition at the interface was achieved and at the triple line a contact angle value of $\theta = 38°$ was shown and kept constant until the end of the experiment. After 15 minutes, the Si/GC couple was fast cooled down to the room temperature and the typical conical angle at the top of the solidifying drop, was observed (Figure 2b).

Preprints (www.preprints.org) | NOT PEER-REVIEWED | Posted: 14 February 2020 doi:10.20944/preprints202002.0188.v1

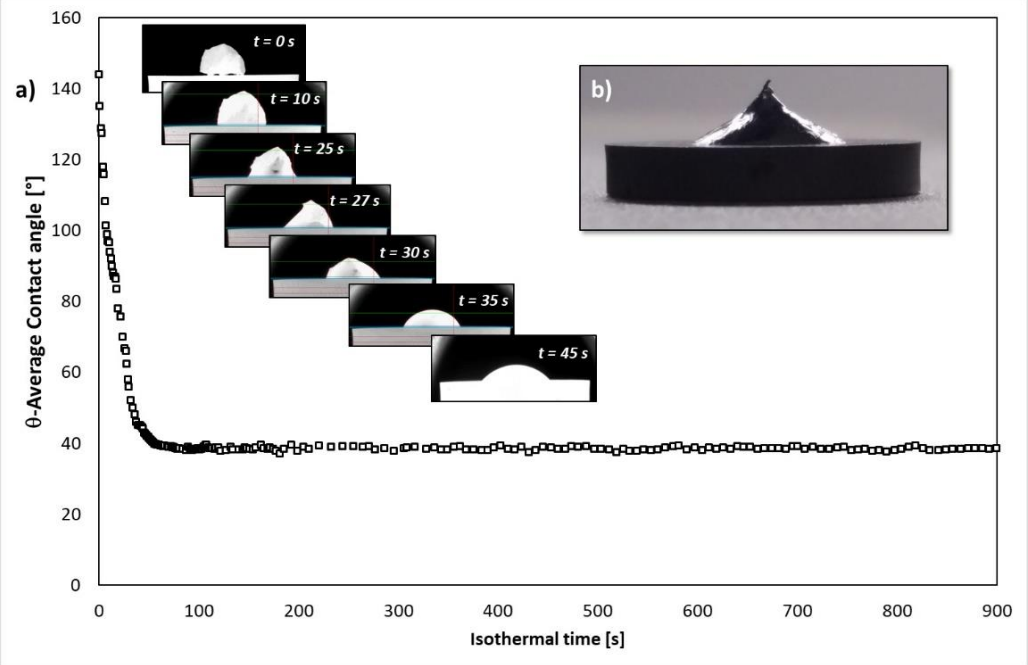

Figure 2. Wettability of GC by liquid Si in contact (□) at T = 1450°C under an Ar atmosphere for 15 minutes: (**a**) contact angle behavior and time sequence of Si-drop spreading on GC; (**b**) Si/GC sample after the wetting experiment.

Depending on the distance from the Si/GC triple line, different microstructures are developed, as shown in Figure 3. Specifically, the presence of a thin SiC layer, was found close to the drop perimeter. Contrarily, moving far from the triple line, circular SiC nodules are well distinguished.

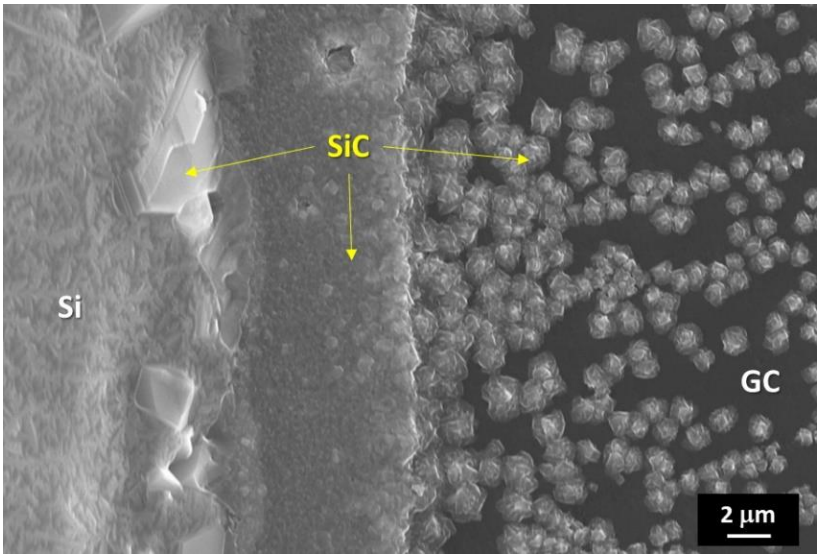

Figure 3. SEM image and EDS analysis performed on the Si/GC couple at the triple line-top drop and after the wetting test performed at T = 1450°C and under an Ar atmosphere for 15 min.

Individual SiC-crystals epitaxially grown up to a size of 5-7 µm were detected at the Si/GC triple line, as shown in Figure 4. In contrast, moving to the middle of the drop, at the cross-section of the Si/GC sample, it is possible to easily identify the interface that is typical of wettability evolving by reactive mechanism. Namely, C-dissolution pockets at the bottom and a compacted layer of SiC-crystals with a size varying from 2 to 5 µm, were revealed (Figure 4b).

Preprints (www.preprints.org) | NOT PEER-REVIEWED | Posted: 14 February 2020 doi:10.20944/preprints202002.0188.v1

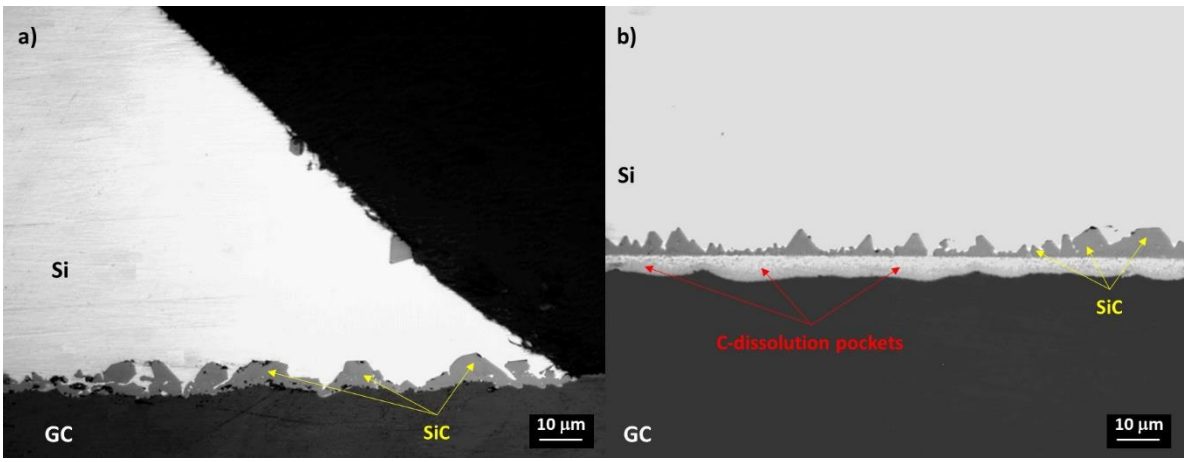

Figure 4. Images at the cross-sectioned Si/GC sample by Optical Microscope after the wetting test performed at T = 1450°C and under Ar atmosphere for 15 minutes: (**a**) triple line (**b**) middle of the sample

In Figure 5, the evolution over time of the contact angle behaviors of the Si-5Zr/GC and Si-15Zr/GC systems, are shown and compared with the wetting behaviour displayed by the liquid Si-27Zr alloy in contact with the same substrate under the same operating conditions [31].

As it can be observed, the achievement of the equilibrium conditions seemed to be not influenced by the different Si-content and the wetting kinetics were almost overlappen (Figure 5b). However, a slight influence of Si-content in the final contact angle value, deserves to be pointed out (Figure 5a). Specifically, contact angle values of θ = 44, 41 and 38° were measured after 15 minutes at the Si-27Zr/GC, Si-15Zr/GC and Si-5Zr/GC triple lines, respectively. It is worth to be highlighted the irregular wetting behaviour exhibited by the Si-27Zr/GC system within the first 40 s respect to the other two systems investigated was observed as it is shown in Figure 6b.

In Figure 6, BSE/EDS analyses performed both at the top drops and at the triple lines of the Si-5Zr/GC (Figures 6a and b) and Si-15Zr/GC (Figure 6d and e) samples processed at T = 1450 °C for 15 minutes, are shown. The presence of SiC-crystals with a size ranging from 2 to 10 µm were found delimiting the drops perimeter. Similarly to the Si/GC couple processed at the same testing temperature, a thin layer of SiC surrounding the drop perimeter at the triple line, was found. In particular, moving far from the triple line, unreacted regions of the GC with over-layered circular and narrowing areas of SiC are well distinguished. Moreover, owing to the applied fast cooling of the samples at the end of the wetting experiment, a crack at the interface was observed.

At the cross-sectioned samples, a fragmented SiC-layer with a thickness of 5-7 µm grown at both triple lines (Figures 6b and c) was detected. Moving toward the middle of the drop, different microstructures were observed, as shown in Figures 6c and 6f. In particular, individual SiC-crystals and C-dissolution pockets were detected at the Si-15Zr/GC interface. Contrarily, an alternating microstructure of thick compact SiC-layers and C-dissolution pockets in contact with the Si-Zr alloy, were found at Si-5Zr/GC system.

Preprints (www.preprints.org) | NOT PEER-REVIEWED | Posted: 14 February 2020 doi:10.20944/preprints202002.0188.v1

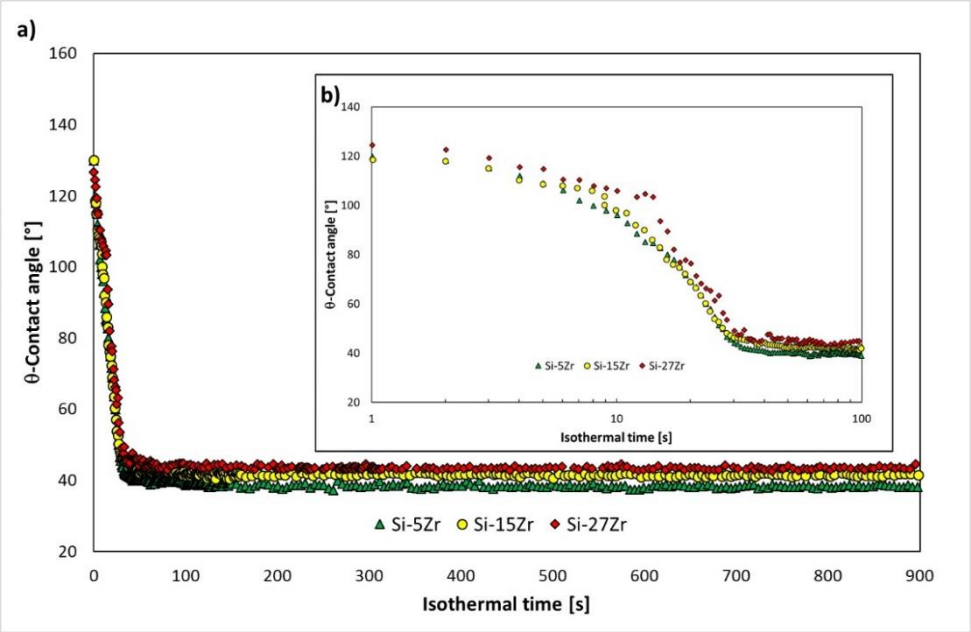

Figure 5. Contact angle behaviors observed at T = 1450°C under an Ar atmosphere for (**a**) 900s and (**b**) 100s as a function of Si-content: (◆) Si-27Zr/GC (●) Si-15Zr/GC and (▲) Si-5Zr/GC.

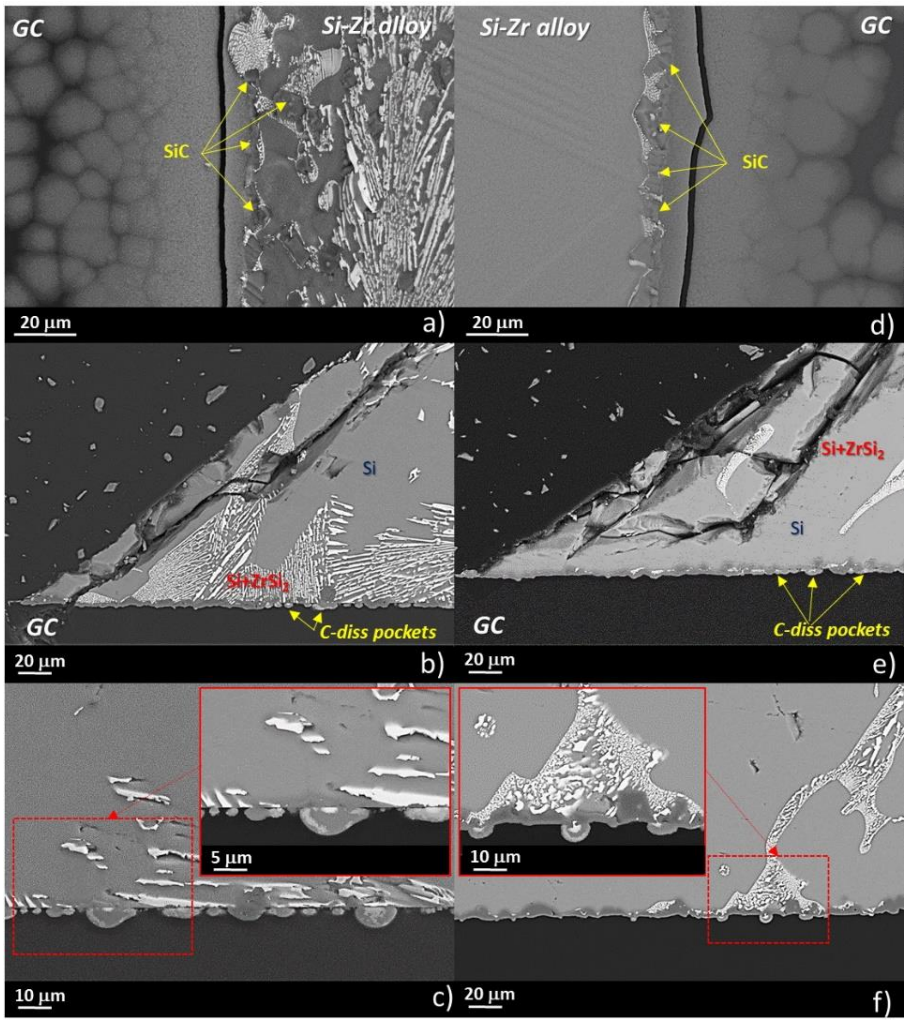

Figure 6. BSE/EDS analyses performed at different magnifications at the triple lines and at the interfaces of the (**a**), (**b**), (**c**) Si-15Zr/GC and (**d**), (**e**), (**f**) Si-5Zr samples after the wetting tests performed at T = 1450 °C for 15 minutes.

 doi:10.20944/preprints202002.0188.v1

4. Discussion

As pointed out in the previous section, an anomalous wetting kinetics, due to a delay in achieving the complete melting of the sample at the liquid Si/GC interface, was observed (Figure 2). Such behavior is typically noticed during wetting tests performed by the contact heating sessile drop experiments [35] and it is caused by the presence of a SiO_2-native oxide layer at the metal surface. However, the native oxide should be decomposed by the following reaction (1) [36]:

$$SiO_{2(s)} + Si_{(l)} \rightarrow 2SiO_{(g)} \uparrow \quad (1)$$

When the SiO_2-layer completely disappears at the interface, liquid Si is able to interact with the GC substrate according to the following exothermic reaction (2):

$$Si_{(l)} + C_{(s)} \rightarrow SiC_{(s)} \quad (2)$$

Indeed, a compact layer of SiC was found at the interface (Figure 4). Additionally, the packaging of SiC-crystals at the interface was already achieved in 15 minutes, which prevents the further interaction phenomena between unreacted C and liquid Si. On the basis of such evidences, the equilibrium at the interface, can be assumed.

After 85 s from the start of the isothermal time, the measured contact angle value of $\theta = 38°$ is in very good agreement with the literature data reported for the liquid Si in contact with the amorphous C and with SiC [37]. In this regard, the wetting of C by liquid Si and Si-based alloys is driven by a combination of reactive and non-reactive mechanisms, as described in [36]. In addition, the equilibrium contact angle exhibited at the triple line is actually resulting from the interaction phenomena occurring between the metal phase and the already produced interfacial SiC layer (reaction 2). Moreover, as widely explained by [38], the wettability of liquid Si and Si-based alloys in contact with C-materials evolves through different spreading stages. Within the first stage (lasting few seconds), C-dissolution and reaction between C and liquid Si, resulting in the appearance of a SiC-thin layer, are the main interaction phenomena taking place at the interface. Subsequently, a decrease in the reactivity is observed due to the aggregation of individual SiC- crystals grown up at the interface actually impeding the direct contact between the reacting phases (i.e. liquid Si and C).

The further advancing of the triple line is favored by the growth of a thin layer of SiC beyond the drop perimeter. It is resulting from evaporation/condensation phenomena of liquid Si onto the unreacted C substrate, as shown in Figure 3.

It worth to be highlighted that the final contact angle values reported in the present work are in good agreement with the value measured at the Si-27Zr/SiC and with the contact angle shown by the dispended drop method [30]. Such outcome let us to conclude that the wetting kinetics and related interfacial phenomena occurring at the Si/GC interface were affected by the presence of SiO_2 segregated at the interface, only during the early stage of the experiment.

As already introduced, a previous study focused on the wetting characteristics of the liquid Si-27Zr in contact with GC [31] and SiC [30] as function of operating conditions (i.e. temperature and time) and method applied was done. Namely, the interfacial phenomena observed in terms of the contact angle behavior, the reactivity, spreading kinetics and microstructural evolution, were analyzed.

Preprints (www.preprints.org) | NOT PEER-REVIEWED | Posted: 14 February 2020 doi:10.20944/preprints202002.0188.v1

In Table 1, the final contact angle values and spreading rates observed at the triple lines as functions of temperature and time are reported and compared with the results provided in the present work.

Table 1. Equilibrium contact angle values (θ_f) and spreading rates (U_{spread}) measured for the liquid Si-rich Si-Zr in contact with GC and SiC as a function of temperature and time by the contact heating sessile drop method: (*) [30] and (**) [31].

System	T [°C]	t [min]	$\theta_f \pm 2$ [°]	U_{spread} [μm/s]
Si-27Zr/GC**	1354	15	51-52	13.9
	1400	15	49	22.7
	1450	15	43	29.7
	1450	45	45	28.6
Si-27Zr/SiC*	1360	15	40	40
	1450	15	38	75
Si-15Zr/GC	1450	15	41	36.4
Si-5Zr/GC	1450	15	38	37.7
Si/GC	1450	15	38	26

The interfacial phenomena occurring at the formed interface between the liquid Si-27Zr alloy and the GC were widely described in [31]. By summarizing, the reactive wetting was defined as the main interaction mechanism taking place when the liquid Si-Zr alloy is in a contact with the amorphous C. It is confirmed by analyzing the spreading rates reported in the Table 1 and Figure 7. Specifically, the achievement of U_{spread} (1354 °C) < U_{spread} (1400 °C) < U_{spread} (1450 °C), is expected. Additionally, the final contact angle values exhibited after 15 minutes between the liquid Si-Zr alloy and the GC at the three different temperatures were obeyed to θ_f (1354 °C) > θ_f (1400 °C) > θ_f (1450 °C), as shown in Figure 7b. The predominance of reactivity as the mechanism controlling the wettability between liquid Si-27Zr alloy and GC is also confirmed by the resulting value of the activation energy of E_a= 222 kJ/mol, that was calculated using the Arrhenius plot of the spreading velocity (Figure 8a) which typically describes reactive mechanisms [36].

The results concerning interaction phenomena observed at the Si-27Zr/GC interface as the function of operating condtions above these overviewed, mainly in terms of spreading rates and measured final contact angle values, can be easily explained by taking into account the fact that all the kinetics related to reactive, diffusion and dissolution phenomena, as well as the evaporation tendency of the liquid metal phase, are enhanced when the temperature is increased.

The influence of the temperature on the final contact angle value was also directly revealed at the Si-27Zr/SiC triple line, as shown in Figure 7c. Additionally, as compared to the behaviour observed for the GC under the same operating conditions, U_{spread} (GC) < U_{spread} (SiC) was a further evidence that the GC is "less" wettable substrate than SiC. Moreover, the θ_f (SiC) < θ_f (GC) is caused by the rougher surface produced by the reaction at the Si-27Zr/GC interface. In particular, the "dewetting phenomenon" is more evident for a time longer than 15 minutes (45 minutes) and the increase of the size of the SiC-crystals from 2-5 to 2-10 μm determined the increase of the final contact angle value from 43 to 45°, as reported in [30].

Preprints (www.preprints.org) | NOT PEER-REVIEWED | Posted: 14 February 2020 doi:10.20944/preprints202002.0188.v1

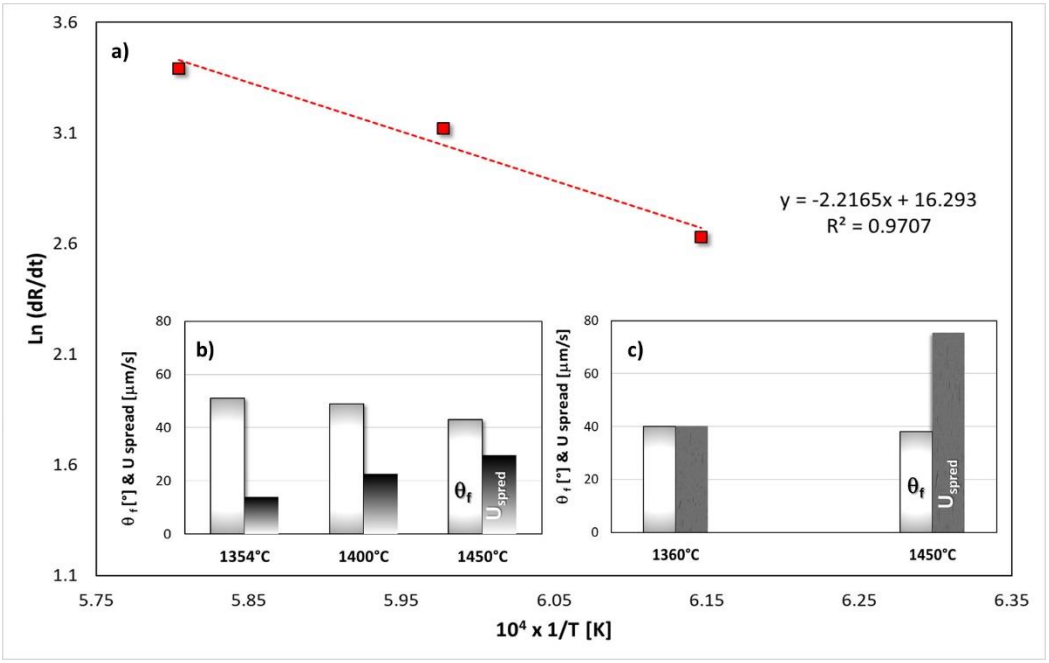

Figure 7. Spreading kinetics in the liquid Si-27Zr/GC system: (a) Arrhenius plot of the spreading rates observed at different testing temperatures; Spreading rates and equilibrium contact angle values as a function of temperature in the (**b**) Si-27Zr/GC and (**c**) Si-27Zr/SiC systems.

By taking into account the interfacial phenomena and the appearance of SiC as the reaction interlayer between Si-Zr alloy and GC before the achievement of equilibrium conditions, the contact angle values measured at the Si-27Zr/GC interface are comparable and in a very good agreement with the literature data. In fact, considering the little difference in Zr-content, the final/equilibrium contact angle values measured at the Si-27Zr/GC triple lines as a function of temperature are in a good agreement with the values measured for the Si-22Zr/GC system (i.e. Si-8at%Zr/GC) under an Ar atmosphere by [32]. Similarly, the reported contact angle values are weakly influenced by increasing of temperature from 1404°C (as it comes from the detected Si-Zr/GC melting point) to 1450°C. Furthermore, during the heating of the sample, the contact angle value increased from 44° to 45°. It can be justified by the growth of SiC crystals at the interface determining the increase of the roughness at the GC-surface.

At T = 1452°C, the contact angle value sharply decreased from 45° to 29° and then remained constant throughout the experiment at 1500°C. In agreement with the authors' interpretation, the interaction phenomena occurring at the interface were affected most probably by the surface oxidation. In fact, during the wetting experiments, the Si-Zr alloy/substrate couples were sourronded by an Al_2O_3 tube which may start to be more permeable and to release oxygen at high temperatures [40].

On the other hand, as above mentioned, under an atmosphere of reduced O_2-content, further oxidation and oxygen transport phenomena at the alloy surface should be suppressed by the presence of counter flows of volatile SiO mono-oxides [41, 42]. In addition, the appearance of stable oxides at the surface is also limited by the high evaporation tendency of liquid Si [40]: condensed Si and Si-oxide "fogs", acting as a barrier and rejecting the O_2-flow coming from the atmosphere to the alloy surface, may be present in the gas phase surrounding the drop.

In the present work, the samples were heated by induction and sourronded by a graphite tube, as described in the section 2. Although the experiment were performed under an Ar static atmopshere, the residual oxygen content (< 0.1 ppm) was further decreased by the following reactions set:

$$C_{(s)} + O_{2(g)} \rightarrow CO_{2(g)} \quad (3)$$

$$2C_{(s)} + O_{2(g)} \rightarrow 2CO_{(g)} \quad (4)$$

$$2CO_{(g)} + O_{2(g)} \rightarrow 2CO_{2(g)} \quad (5)$$

Preprints (www.preprints.org) | NOT PEER-REVIEWED | Posted: 14 February 2020 doi:10.20944/preprints202002.0188.v1

$$CO_{2\,(g)} + C_{(s)} \rightarrow 2CO_{(g)} \quad (6)$$

In particular, under thermodynamic considerations, at the testing temperature of T = 1450°C, the reaction 4 is one of most favoured. In addition, if the mentioned reactions are concomitant with the release of SiO monoxide, as mentioned above typically occurring during the SiO_2 decomposition, the following reactions may take place:

$$SiO_{(g)} + CO_{(g)} \rightarrow SiC_{(s)} + O_{2\,(g)} \quad (7)$$
$$SiO_{(g)} + 3CO_{(g)} \rightarrow SiC_{(s)} + 2CO_{2\,(g)} \quad (8)$$
$$SiO_{(g)} + 2C_{(s)} \rightarrow SiC_{(s)} + CO_{2\,(g)} \quad (9)$$

The reactions listed above belong to the set of equilibria responsible of the growth of SiC micro and nanowires on C and SiC (seeds) via vapour-solid process, as reported in [43, 44, 45, 46]. This type of growth is widely used to produce high quality SiC whiskers. The growth of SiC-crystals along the [111] direction is resulting from the spiral-overlayering of hexagonal SiC planes. The final SiC-wires morphology strongly depends on the process parameters, specifically its temperature, starting materials and atmosphere, which in other words control the SiO-supersaturation level into the vapour phase. The temperature imposed to promote the growth from nano to micro-SiC wires typically ranges from 1400 to 1600 °C. In addition, depending on the operating conditions, the process time takes at least 30 minutes in order to detect the appearance of the first measurable SiC nanowires.

In the present case, the presence of SiC micro-crystals grown up at the surface of epitaxial SiC crystals, in turn generated from the reaction (2), were detected at the triple line of the Si-27Zr/GC sample processed for 45 minutes, as shown in Figures 8a and 8b.

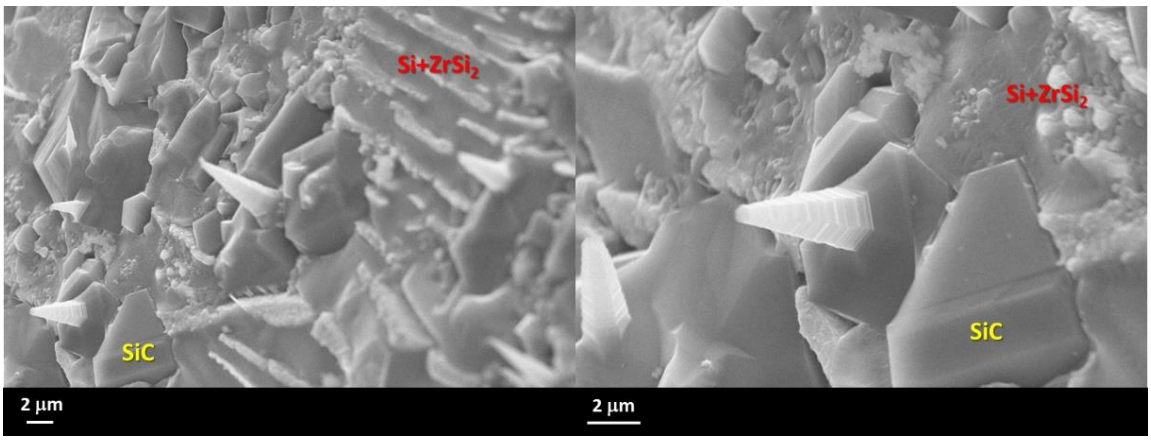

Figure 8. SEM/EDS analyses performed at tow different magnifications near the triple line of the Si-27Zr/GC sample after the wetting tests performed at T = 1450 °C for 45 minutes.

The appearance of SiC-wires at the alloy drop surface confirms that within the performed wetting experiments, the sample was under deoxidation condition since the increase of SiO partial pressure into the experimental environment (by reaction (2)), combined with the presence of CO, was high enough to promote the vapour-solid process for growing the detected SiC nano/micro-crystals.

The collected results on wetting characteristics and spreading kinetics reported in Table 1, are consistent with the effect of Si-content.

As pointed out in the previous section, the wetting behaviour exhibited by the Si-27Zr/GC system within the first 40 s respect differs from the other two systems investigated, as shown in Figure 5b. The irregular wetting kinetics may be caused by the presence of higher melting $ZrSi_2$ precipitates (Tm $ZrSi_2$ = 1620°C [47]) at the bottom of the sample (Figure 1f) embedded into the eutectic matrix and even at the surface of alloy drop.

Preprints (www.preprints.org) | NOT PEER-REVIEWED | Posted: 14 February 2020 doi:10.20944/preprints202002.0188.v1

The weak influence of the alloy composition on the spreading rate is reasonable if the very limited range of Si-content (i.e. 0-10at%) is considered. It can be also envinced by the comparable value of spreading rates observed at T = 1450°C. However, on the measured wetting characteristics, a "more pronounced" effect of the Si-content can be found in terms of the measured final contact angle value and consequently, the trend of wettability seems to be improved by increasing the Si-content into the alloy.

According to the thermodynamic calculation of the C-Zr-Si ternary phase diagram reported in [39], Si-rich Si-Zr alloys with a Zr-molar fraction up to X = 0.17, should be in equilibrium with Si and SiC phases. In fact, except the presence of SiC at the interface, no any other compounds as reaction product were detected, as shown in Figure 9. In addition, by comparing the SEM/EDS analyses performed on the cross-sectioned samples, similar developed microstructures were found at the Si-5Zr/GC and Si-27Zr/GC interfaces both at the triple lines and in the middle of the samples. In particular a more compacted SiC layer at the triple line, was found, as expected [36]. Contrarily, in the middle of the drop, the equilibrium conditions were not yet achieved. Indeed the presence of well-distinguished C-dissolution pockets were still noted. The different behaviour exhibited at the interface by the liquid Si-Zr alloys processed at T = 1450°C respect to pure Si, it is most probably caused by the presence of Zr as alloying element.

Finally, he results obtained in terms of slight composition-dependency regarding the wetting characteristis and on the interface developed microstructures obtained under the same experimental conditions are in good agreement with similar investigations performed on other Si-based systems by the authors [27, 29].

In the view of providing new knowledge for optimizing the infiltration process used to fabricate SiC/ZrSi2 composites, liquid Si-Zr alloys enriched in Si respect to the Si-27Zr alloy that are usually selected as infiltrant, may not enhance the pore closure phenomenon. On the other hand, the use of Si-Zr alloys with higher Si content should be limited to avoid the decreasing of the overall thermo-mechanical response of thee produced composites.

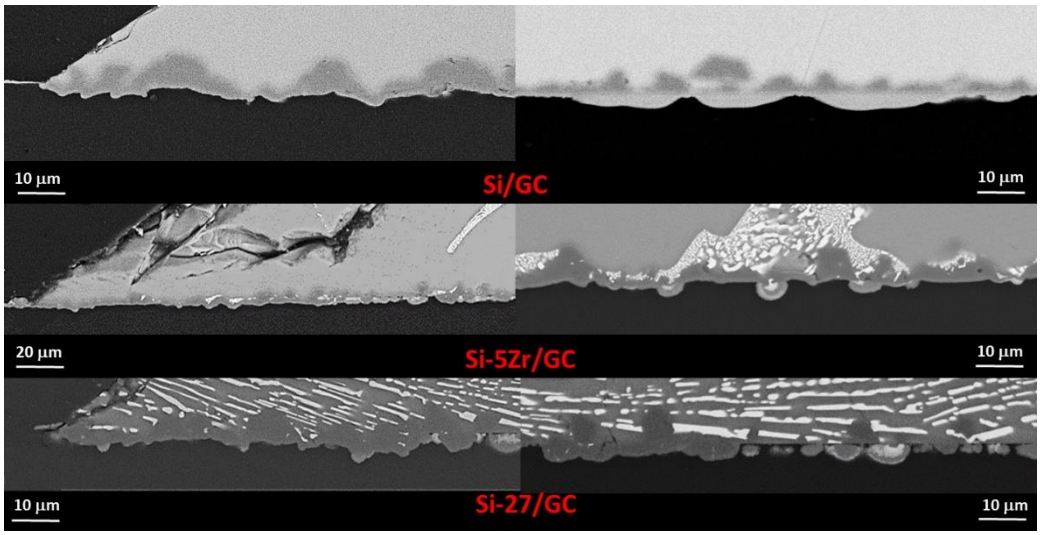

Figure 9. BSE/EDS analyses performed at different magnifications at (**a**) the triple lines and at (**b**) the interfaces close to the middle of the Si/GC, Si-5Zr/GC and Si-27Zr/GC samples after the wetting tests performed at T = 1450 °C for 15 minutes.

5. Conclusions

A comprehensive study of the interaction phenomena occurring when a liquid Si-rich Si-Zr alloy is in contact with the amorphous C was done and the more relevant findings are provided. In

particular, a careful analysis of the contact angle behaviors, spreading kinetics, reactivity and interfacial developed microstructures as a function of the alloy composition at T = 1450°C, were done.

It was documented that the wettability of GC by Si-rich Si-Zr alloys is controlled by the reactive mechanism.

Despite the pronounced reactivity, the wetting characteristics are slightly composition-dependent and the overall phenomena are controlled by the growing and thickening of SiC crystals at the interface.

The wetting characteristics and spreading kinetics observed at the Si-rich Si-Zr alloys/GC triple lines at T = 1450°C are in a very good agreement with the results obtained from previous investigations performed on Si-27Zr/GC and Si-27/SiC systems.

In the view to provide knowledge for optimizing the infiltration process used to fabricate SiC/$ZrSi_2$ composites, liquid Si-Zr alloys enriched in Si respect to the Si-27Zr alloy usually selected as infiltrant, may not enhance the pore closure phenomenon.

On the other hand, the use of Si-Zr alloys with the Si content exceeding that of the eutectic composition should be limited in order to avoid the decreasing of the overall thermo-mechanical response of the produced composite.

Author Contributions: All authors have read and agree to the published version of the manuscript. Conceptualization, D.G., W. P., and J.N.; methodology, D.G. and A.K.; software, D.G., G.B. and A.K.; validation, D.G., W.P. and J.N.; formal analysis, D.G. and W.P.; investigation, D.G, G.B. and A.K.; writing—original draft preparation, D.G.; writing—review and editing, D.G., W. P. and J.N.; supervision, J.N.

Acknowledgments:
The work performed by DG, W.P, G.B. and A.K. was supported by National Science Center of Poland through POLONEZ project number UMO-2016/23/P/ST8/01916. This project is carried out under POLONEZ-3 program which has received funding from European Union's Horizon 2020 research and innovation program under Marie Skłodowska-Curie grant agreement. No 665778.

The work in part performed by JN was funded by the Spanish "Ministerio de Economía y Competitividad" (Grant MAT2017-86992-R), and action Mobility of Alicante University.

DG wishes to thank Prof. Alberto Passerone for fruitful discussion and Dr Rada Novakovic for critical reading and suggestions provided to improve the paper. DG is grateful to Mr Francesco Mocellin for his technical assistance.

Conflicts of Interest: The authors declare no conflict of interest.

References

1. Miracle, D.B., Light-weighting and the Future of Aerospace Metals. In: *Light Weighting for Defense, Aerospace, and Transportation*. A. A. Gokhale et al. (Eds.), Indian Institute of Metals Series, Springer Nature Singapore Pte Ltd., 2019.
2. Zhang, X., Chen, Y., Hu, J., Recent advances in the development of aerospace materials, Progress in Aerospace Sciences **2018**, 97, 22–34.

3. Singh, H., Nrip, S. J., Tyagi, A. K., An overview of metal matrix composite: Processing and SiC based mechanical properties, J. Eng. Res. Stu. **2011**, 2 (4), 72-78.
4. Rosso, M., Ceramic and metal matrix composites: Routes and properties, J. Mater. Process.Tech. **2006**, 175, 364–375.
5. Simonenko, E. P., Sevastyanov, D. V., Simonenko, N. P., Sevastyanov, V. G., Kuznetsov, N. T., Promising Ultra_High_Temperature Ceramic Materials for Aerospace Applications, Russ. J. Inorg. Chem. **2013**, 58 (14), 1669–1693.
6. Mileiko, S.T., Constituent Compatibility and Microstructural Stability, Comprehensive Composite Materials **2000**, 4, 265-287.
7. Siddharth Sharma, A., Fitriani, P., Yoon, D. H., Fabrication of SiCf/SiC and integrated assemblies for nuclear reactor applications, Ceram. Int. **2017**, 43, 17211-17215.
8. Koyanagi, T., Katoh, Y., Nozawa, T., Snead, L.L., Kondo, S., Henager Jr., C.H., Ferraris, M., Hinoki, T., Huang, Q., Recent progress in the development of SiC composites for nuclear fusion applications, J. Nucl. Mater. **2018**, 511, 544-555.
9. Katoh, Y., Snead, L.L., Henager Jr., C.H., Hasegawa, A., Kohyama, A., Riccardi, B., Hegeman, H., Current status and critical issues for development of SiC composites for fusion applications, J. Nucl. Mater. **2007**, 367, 659–671.
10. Murarka. S. P., Transition Metal Silicides, Ann. Rev. Mater. Sci. **1983**, 13, 117-137.
11. Cho, I. J., Park, K.T., Lee, S. K., Nersisyan, H.H., Kim, Y. S., Lee, J.K, Rapid and cost-effective method for synthesizin,g zirconium silicides, Chem. Eng. J. **2010**, 165, 728–734.
12. Le Flem, M., Canel, J., Urvoy, S., Processing and characterization of Zr3Si2 for nuclear applications, J. Alloys Compd. **2008**, 465, 269–273.
13. Ness, J.N., Page, T.F., Microstructural evolution in reaction-bonded silicon carbide, J. Mater. Sci. **1986**, 21, 1377–1397.
14. Whitehead, A.J., Page, T.F., Fabrication and characterization of some novel reaction-bonded silicon carbide materials, J. Mater. Sci. **1992**, 27, 839–852.
15. Caccia, M., Narciso, J., SiC manufacture via reactive infiltration, Processing and Properties of Advanced Ceramics and Composites VI: Ceram. Trans. John Wiley & Sons, **2014**.
16. Caccia, M., Narciso, J., Key parameters in the manufacture of SiC-based composite materials by reactive melt infiltration, Materials **2019**, 12 (15), 2425.
17. Camarano, A., Giuranno, D., Narciso, J., New advanced SiC-based composite materials for use in highly oxidizing environments: Synthesis of SiC/$IrSi_3$, J. Eur. Ceram. Soc. **2020**, 40 (3), 603-611.
18. Esteban, O. C., Caccia, M., Camarano, A., Narciso, J., Advances in High Temperature Ceramic Matrix Composites and Materials for Sustainable Development; Ceram. Trans., John Wiley & Sons, **2017**.
19. Jiang, J., Wang, S., Li, W., Chen, Z., Fabrication of Cf/ZrC–SiC composites using Zr–8.8Si alloy by melt infiltration, Ceram. Int. **2015**, 41, 8488–8493.
20. Tong, Y., Bai, S., Hu, Y., Liang, X., Ye, Y., Qin, Q. H., Laser ablation resistance and mechanism of Si-Zr alloyed melt infiltrated C/C-SiC composite, Ceram. Int. **2018**, 44, 3692–3698.
21. Zhou, Z., Sun, Z., Ge, Y., Peng, K., Ran, L., Yi, M., Microstructure and ablation performance of SiC–ZrC coated C/C composites prepared by reactive melt infiltration, Ceram. Int. **2018**, 44 8314–8321.
22. Tong, Y.G., Cai, Z.H., Bai, S.X., Hu, Y.L., Hua, M.Y., Xie, W., Ye, Y.C., Li, Y., Microstructures and properties of Si-Zr alloy based CMCs reinforced by various porous C/C performs, Ceram. Int. **2018**, 44, 16577–16582.
23. Tsunoura, T., Yoshida, K., Yano, T., Aoki, T., Ogasawara, T., Oxidation mechanisms of SiC-fiber–reinforced Si eutectic alloy matrix composites at elevated temperatures, J. Am. Ceram. Soc., **2019**, 395, 174–569.
24. Novakovic, R., Giuranno, D., Caccia, M., Amore, S., Nowak, R., Sobczak, N., Narciso, J., Ricci, E., Thermodynamic, surface and structural properties of liquid Co-Si alloys. J. Mol. Liq. **2016**, 221, 346–353.
25. Amore, S., Giuranno, D., Novakovic, R., Ricci, E., Nowak, R., Sobczak, N., Thermodynamic and surface properties of liquid Ge-Si alloys, Calphad **2014**, 44, 95-101.
26. Giuranno, D., Tuissi, A., Novakovic, R., Ricci, E., Surface tension and density of Al-Ni alloys, J. Chem. Eng. Data **2010**, 55, 3024–3028.

27. Giuranno, D., Sobczak, N., Bruzda, G., Nowak, R., Polkowski, W., Kudyba, A., Polkowska, A., Novakovic, R., Studying the Wettability and Reactivity of Liquid Si-Ti Eutectic Alloy on Glassy Carbon, J. of Materi Eng and Perform **2019**, 28 (6), 3460-3467.
28. Giuranno, D., Sobczak, N., Bruzda, G., Nowak, R., Polkowski, W., Kudyba, A., Polkowska, A., Novakovic, R., Wetting and Spreading Behavior of Liquid Si-Ti Eutectic Alloy in Contact with Glassy Carbon and SiC at T = 1450 °C, Metall and Mat Trans A **2019**, 50 (10), 4814-4826.
29. Caccia, M., Amore, S., Giuranno, D., Novakovic, R., Ricci, E., Narciso, J., Towards optimization of SiC/$CoSi_2$ composite material manufacture via reactive infiltration: Wetting study of Si–Co alloys on carbon materials, J. Eur. Ceram. Soc. **2015**, 35 (15), 4099-4106.
30. Giuranno, D., Bruzda, G., Polkowska, A., Nowak, R., Polkowski, W., Kudyba, A., Sobczak, N., Mocellin, F., Novakovic, R., Design of refractory SiC/ZrSi2 composites: wettability and spreading behavior of liquid Si-10Zr alloy in contact with SiC at high temperatures, J. Eur. Ceram. Soc. 2019, 10.1016/j.jeurceramsoc.2019.12.027.
31. Giuranno, D., Polkowska, A., Polkowski, W., Novakovic, R., Wetting behavior and reactivity of liquid Si-10Zr alloy in contact with glassy carbon, J. Alloys Compd, **2020** https://doi.org/10.1016/j.jallcom.2020.153643.
32. Naikadea, M., Fankhänel, B., Weber, L., Ortona, A., Stelter, M., Graule, T., Studying the wettability of Si and eutectic Si-Zr alloy on carbon and silicon carbide by sessile drop experiments, J. Eur. Ceram. Soc **2019**, 39, 735-742.
33. Louis, E., Miralles, J.A., Molina, J.M., Reactive infiltration: identifying the role of chemical reactions, capillarity, viscosity and gravity, J. Mater. Sci. **2017**, 52, 7530–7538.
34. Liggieri, L., Passerone, A., An automatic technique for measuring the surface tension of liquid metals, High. Technol. **1989**, 7, 80-86.
35. Eustathopoulos, N., Sobczak, N., Passerone, A., Nogi, K., Measurement of contact angle and work of adhesion at high temperature, J. Mat. Sci. **2005**, 40, 2271-2280.
36. Drevet, B., Eustathopoulos, N., Wetting of ceramics by molten silicon and silicon alloys: a review, J. Mat. Sci. **2012**, 47, 8247–8260.
37. Dezellus, O., Eustathopoulos, N., Fundamental issues of reactive wetting by liquid metals Fundamental issues of reactive wetting by liquid metals, J. Mater. Sci. **2010**, 45, 4256–4264.
38. Voytovych, R., Israel, R., Calderon, N., Hodaj, F., Eustathopoulos, N., Reactivity between liquid Si or Si alloys and graphite, J. Eur. Ceram. Soc. 2012, 32 (14), 3825-3835.
39. Chen., H.M., Xiang, Y., Wang. S., Zheng, F., Liu, L.B., Jin, Z.P., Thermodynamic assessment of the C–Si–Zr system, J. Alloys Compod **2009**, 474, 76–80.
40. Knacke, O., Kubashewski, O., Hesselmann, K., Thermochemical Properties of Inorganic Substances, 2nd ed., Springer Verlag, Düsseldorf, **1991**.
41. Giuranno, D., Arato, E., Ricci, E., Oxidation conditions of pure liquid metals and alloys, Chem. Eng. Trans. **2011**, 24, 571-576.
42. Ratto, M., Ricci, E., Arato, E., Mechanism of oxidation/deoxidation of liquid silicon: Theoretical analysis and interpretation of experimental surface tension data, J. Crys. Grow. **2000**, 217 (3), 233-249.
43. Wu, R., Li, B., Gao, M., Chen, J., Zhu, Q., Pan, Y., Tuning the morphologies of SiC nanowires via the control of growth temperature, and their photoluminescence properties, Nanotech. **2008**, 19, 335602.
44. Adrievski, R. A., Sinthesys, structure and properties of nanosized silicon carbide, Rev. Adv. Mater. Sci., **2009**, 22, 1-20.
45. Milewski, J.V., GAC, F.D., Petrovic, J.J., Skaggs, S.R., Growth of beta-silicon carbide whiskers by the VLS process, J. Mater. Sci. **1985,** 20, 1160-1166.
46. F.J. Narciso-Romero, F. Rodríguez-Reinoso, Synthesis of SiC from rice husks catalyzed by iron, cobalt or nickel, J. Mater. Sci. **1996**, 31, 779-784.
47. Massalski, T.B., Binary alloy phase diagrams, Metals Park, **1986**, OH, ASM.